IEEE Access
Multidisciplinary | Rapid Review | Open Access Journal

Received October 7, 2019, accepted November 4, 2019, date of publication November 25, 2019,
date of current version December 11, 2019.

Digital Object Identifier 10.1109/ACCESS.2019.2955697

Stochastic Optimal Control to Minimize the Impact of Manufacturing Variations on Nanomechanical Systems

YUJI ITO[1], (Member, IEEE), KEITA FUNAYAMA[1], JUN HIROTANI[2], YUTAKA OHNO[2,3], AND YUKIHIRO TADOKORO[1], (Senior Member, IEEE)

[1]TOYOTA CENTRAL R&D LABS., INC., Nagakute 480-1192, Japan
[2]Department of Electronics, Nagoya University, Nagoya 464-8603, Japan
[3]Institute of Materials and Systems for Sustainability, Nagoya University, Nagoya 464-8603, Japan

Corresponding author: Yuji Ito (ito-yuji@mosk.tytlabs.co.jp)

This work was partly supported by JSPS KAKENHI Grant Number JP18K04222.

ABSTRACT This paper presents a control method intended to suppress the effects of manufacturing variations on nanomechanical systems. Often, the resonance characteristics of nanoscale devices are inconsistent, due to unavoidable variations in the fabrication process. This is important because resonant vibrations enhance the sensitivities of the devices. As such, the sensitivities of these systems can be degraded if the device characteristics are not identified. To address this fundamental problem, this paper presents a multidisciplinary method based on control theory, nanotechnology, and communication technology. A stochastic optimal feedback controller is employed to enhance an average sensitivity by regarding the variations as stochastic parameters. This method is applied to nanoscale receivers that detect transmitted binary data based on binary phase-shift keying in communication systems. The proposed method controls the vibrations of carbon nanotubes (CNTs) that serve as the antennas of the receiver. The proposed method is demonstrated via a numerical simulation using nanoscale receivers with the manufacturing variation. The simulation based on experimental data obtained from CNTs shows that the average performance of the devices is enhanced.

INDEX TERMS Nanoelectromechanical systems, optimal control, stochastic systems.

I. INTRODUCTION

Nano- and micro-electromechanical systems (NEMS and MEMS) both represent promising platforms for high sensitivity sensing applications [1]–[7]. Resonant mode vibrations are known to enhance the sensitivity of NEMS/MEMS, and the associated nonlinear behavior can allow signal processing devices to be miniaturized [8]–[14]. However, nanoscale devices are difficult to fabricate exactly as designed, and unavoidable manufacturing variations can cause changes in the various characteristics of NEMS/MEMS, with potentially significant effects on response [15]–[17]. The present work demonstrates a simple control scheme to suppress the effects of such variations. The aim of this process is to secure the desired performance, especially in the case of the future mass-production of NEMS/MEMS.

The associate editor coordinating the review of this manuscript and approving it for publication was Ton Do.

Variation in these devices is often found in geometrical properties, such as length and width, and/or the mass of the vibrating point [15]–[17]. A typical example is presented in Fig. 1, which shows a nanoscale cantilever (Fig. 1(a)) formed from a multi-walled carbon nanotube (CNT) on a SiO_2 wafer, together with electrodes produced using electron beam lithography. Unfortunately, in the case of the fabricated samples shown in Fig. 1(b), the cantilever length, L, and the gap, h_0, between the CNT tip and the anode are significantly different from the design. The statistical variations are summarized in Fig. 1(c), based on the distributions of the two parameters among 108 fabricated samples. The fabrication method is found in [18].

There have been many attempts employing control methods to achieve the required level of performance in such devices. Unfortunately, the methods require the tuning of controllers based on training sequences (see details in Section II). Thus, it would be desirable to design

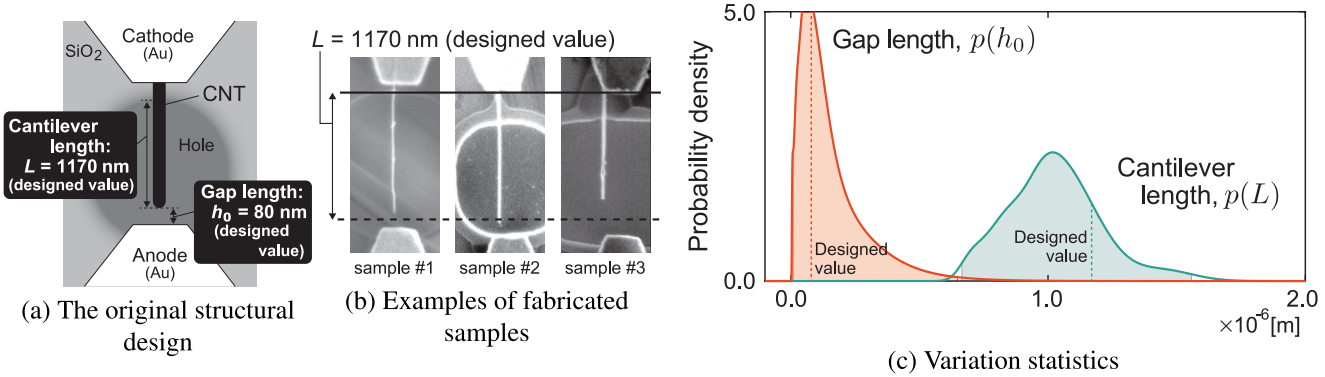

(a) The original structural design

(b) Examples of fabricated samples

(c) Variation statistics

FIGURE 1. An example of variations from design in a nanomechanical system. A CNT cantilever was designed (a) and 108 samples were fabricated using a semiconductor process. Typical specimens of this device demonstrating production variation are presented in (b) and the statistical variations are summarized in (c).

controllers for the devices that do not require costly tuning processes.

The present work provides a simple control method intended to suppress the effects of manufacturing variations on nanomechanical systems. The proposed method is based on our framework that exploits the statistics of stochastic parameters [19]. Essentially, a parameter affected by manufacturing variation can be treated as a stochastic parameter because the variations result from an unpredictable process and/or environment. Although the exact value of the parameter for each device may be unknown, statistics such as those in Fig. 1(c) can be obtained based on taking measurements from a sample of the fabricated devices. Following such measurements, a feedback gain associated with the proposed control method is calculated from the statistics. This technique results in a simple method because the gain can be preset such that a tuning process is not required.

The remainder of this paper is organized as follows. Section II reviews other control approaches related to this subject. Section III describes a generalized problem that is the focus of this paper. As a means of addressing the stated problem, Section IV presents the proposed method, which is based on our stochastic control method [19]. The proposed method is applied to a nanoscale receiver [11] in Section V. A numerical simulation based on experimental data obtained from CNTs is performed to evaluate the proposed method in Section V-C. Finally, conclusions are presented and future work is discussed in Section VI.

II. LITERATURE REVIEW

Control methods intended to allow NEMS/MEMS to exhibit the required level of performance are herein briefly reviewed. One prior study researched means of controlling resonator vibrations in nanomechanical systems, exhibiting manufacturing variations [20]. Along with optimal control criteria [21], a variety of methods focusing on the control of microscopic systems have been investigated [22]. These techniques often incorporate a feedback control framework that is effective if the feedback gain is optimized via tuning with a training sequence [23]–[25]. However, these procedures are extremely costly because of the tuning systems involved. In contrast to these previous approaches, our proposed method can preset a feedback gain without requiring tuning.

Our method presented in this paper is developed based on our stochastic optimal control theory [19]. This theory focuses on linear dynamical systems with time-invariant stochastic parameters. Controlling the systems with such parameters is as an important topic in the field of control theory (e.g., [26]–[28]). The time-invariant stochastic parameters associated with this theory are defined as static random variables that do not vary depending on time. This time-invariant characteristic is well-suited to the representation of manufacturing variations in physical parameters. Various control methods have also been proposed for time-varying stochastic parameters (e.g., [29]–[34]). Parameters that vary over time are applicable to cases in which noise has an effect on the parameters, in contrast to static manufacturing variations. Also, some types of the time-varying stochastic parameters are independent and identically distributed. Such a property simplifies control problems compared with those of the time-invariant parameters. Although several methods [29], [35] may treat both types of stochastic parameters, the designed controllers are not state feedback laws or the parameters are assumed to be observable. The method [19] employed in the present paper can design state feedback controllers even for unobservable stochastic parameters.

III. PROBLEM STATEMENT

The problem to be addressed in this paper is described herein in a general form based on the equation of motion for a nanomechanical system. In addition, to simplify the discussion, we focus on a linear vibrational mode. The vibration is excited by a force $f(t)$ that is continuous and periodic with the period $T_f > 0$. This vibration is characterized by the linear equation:

$$\tilde{m}\ddot{x} + \tilde{\gamma}\dot{x} + \tilde{k}x = f - u(t), \tag{1}$$

where x is the oscillator coordinate, $\tilde{m}$ is the effective mass, $\tilde{\gamma}$ is the friction coefficient, and $\tilde{k}$ is the spring constant [36]. The notation $\tilde{}$ indicates a stochastic parameter. The three parameters $\tilde{m}$, $\tilde{\gamma}$ and $\tilde{k}$ take bounded positive values that are unknown and also stochastic because of manufacturing variations. The motion reflected in x is unpredictable due to its dependence on the stochastic parameter $\alpha := [\tilde{m}, \tilde{\gamma}, \tilde{k}]$. To reduce the effect of the variations, we employ feedback control by adding the input variable u.

Traditional control theory states that the feedback gain, which is included in the control input, can be determined by maximizing a performance index [21]. This index, which is denoted herein as J, depends on both the input and the state variable of the system. In the case of (1), the state variable is the coordinate x. Hence, the index can be written as:

$$J_\alpha(u) = \frac{1}{T}\int_0^T \phi(x_\alpha)\mathrm{d}t, \tag{2}$$

where ϕ is a continuously differentiable predefined function and T is the focused time interval. The subscript α indicates that the corresponding variable/function is affected by the stochastic parameter. The form of (2) allows us to consider various types of performance indices because the choice of the function ϕ determines the physical meaning of the index. As an example, $J_\alpha(u)$ represents a power (mean square) of a periodic x when $\phi(x) = x^2$ and T is the period of x.

Unfortunately, when maximizing the index $J_\alpha(u)$, two difficulties are associated with calculating the index. One issue is that the index depends on the unknown parameter α, which means that the value of the index is difficult to compute. In addition, the calculation is affected by the form of the control input. As an example, employing a nonlinear form with higher-order terms of the state variable would result in difficulty in finding the optimal gain.

IV. PROPOSED METHOD

In this section, we propose a control method for nanomechanical systems to solve the problem stated in Section III. Section IV-A presents an overview of the proposed method. The proposed method requires the use of two techniques to estimate the probability distribution of the stochastic parameter α and to solve an optimization problem regarding the control input u. The two techniques are described in Sections IV-B and IV-C. Finally, stability and robustness for the proposed control method are analyzed in Section IV-D.

A. OVERVIEW

The proposed method addresses the two difficulties noted in the last paragraph of Section III. To mitigate the first issue, we focus on the optimization of an average value. Specifically, the expected value of $J_\alpha(u)$ with respect to α. The optimal feedback input is then determined using the maximization:

$$\max_u \int_\alpha p(\alpha) J_\alpha(u)\mathrm{d}\alpha. \tag{3}$$

Data-driven approaches estimate the probability density function (PDF) $p(\alpha)$ of α based on the measurement data obtained from actual test samples. Example of estimated PDFs are presented in Fig. 1(c). The details of the method used to estimate the PDF are provided in Section IV-B.

An approximate solution to the optimization problem (3) can be obtained based on our stochastic optimal control theory [19]. Fortunately, this theory also solves the second problem, by allowing the control input to be expressed in terms of the linear equation:

$$u_{\mathrm{L}}(x, \dot{x}) = k_{\mathrm{g}} x + \gamma_{\mathrm{g}} \dot{x}, \tag{4}$$

where k_{g} and γ_{g} are the feedback gains, both of which should be optimized. The controller in (4) is applied to the input u of the oscillator in (1). After transposing $u(t)$ in (1), substituting $u(t) = u_{\mathrm{L}}(x(t), \dot{x}(t))$ and (4) into (1) yields the following feedback system:

$$\tilde{m}\ddot{x} + (\tilde{\gamma} + \gamma_{\mathrm{g}})\dot{x} + (\tilde{k} + k_{\mathrm{g}})x = f. \tag{5}$$

Let us assume that $k_{\mathrm{g}} > -\tilde{k}$ and $\gamma_{\mathrm{g}} > -\tilde{\gamma}$ are satisfied for any $\alpha = [\tilde{m}, \tilde{\gamma}, \tilde{k}]$. Stability and robustness of the feedback system (5) are then guaranteed that are shown in Section IV-D.

The optimization problem (3) is considered with regard to the feedback system (5). Unfortunately, straightforward calculation of the performance index $J_\alpha(u_{\mathrm{L}})$ is computationally difficult because $J_\alpha(u_{\mathrm{L}})$ contains the integral $\int_0^T \ldots \mathrm{d}t$, as shown in (2). Based on the form of the feedback system (5), the index $J_\alpha(u_{\mathrm{L}})$ can be approximated using a simple function. Recall that $f(t)$ is continuous and periodic with the period T_f. If $f(t) = 0$ for any t, the feedback system (5) has no periodic solution apart from the trivial one ($x(t) = 0$) because $(\tilde{\gamma} + \gamma_{\mathrm{g}}) > 0$ and $(\tilde{k} + k_{\mathrm{g}}) > 0$ for any α. Consequently, there exists a unique periodic solution $\bar{x}_\alpha(t)$ with the period T_f to the feedback system (5) that satisfies $\bar{x}_\alpha(t) = \bar{x}_\alpha(t + T_f)$ [37, Theorem 2.1.1]. Using this periodic solution, in the case that $T = sT_f$ for a natural number $s \in \{1, 2, \ldots\}$, the index $J_\alpha(u_{\mathrm{L}})$ can be suitably approximated by:

$$\begin{aligned} J_\alpha(u_{\mathrm{L}}) &\approx \hat{J}_\alpha(u_{\mathrm{L}}) := J_\alpha(u_{\mathrm{L}})|_{x_\alpha = \bar{x}_\alpha, T = T_f} \\ &= \frac{1}{T_f}\int_0^{T_f} \phi(\bar{x}_\alpha|_{u=u_{\mathrm{L}}})\mathrm{d}t. \end{aligned} \tag{6}$$

The approximated index $\hat{J}_\alpha(u_{\mathrm{L}})$ can be readily calculated by considering the periodic solution $\bar{x}_\alpha$ with the single period T_f. The approximation in (6) is based on our prior work [38], and the derivation of this approximation is provided in Appendix.

The proposed control method is summarized in Fig. 2 and Algorithm 1. For the stochastic parameter α that is affected by the manufacturing variation, the PDF $p(\alpha)$ can be obtained by measurements of test samples. Based on the resulting information, the two sub-optimal feedback gains $\breve{k}_{\mathrm{g}}$ and $\breve{\gamma}_{\mathrm{g}}$ are calculated by solving the optimization problem:

$$(\breve{k}_{\mathrm{g}}, \breve{\gamma}_{\mathrm{g}}) = \arg\max_{k_{\mathrm{g}}, \gamma_{\mathrm{g}}} \int_\alpha p(\alpha)\hat{J}_\alpha(u_{\mathrm{L}})\mathrm{d}\alpha. \tag{7}$$

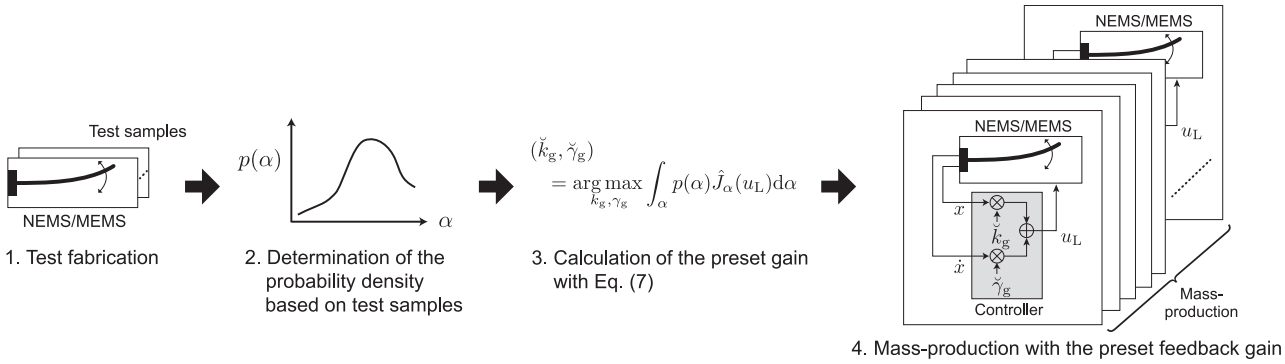

FIGURE 2. Proposed control framework for manufacturing variations.

Algorithm 1 Stochastic Optimal Control to Suppress the Manufacturing Variation in a Nanomechanical System

Input: N fabricated samples of a nanomechanical system

Output: Mass production of the nanomechanical system controlled using the preset of feedback gains

1: Definiton of the stochastic parameter α (e.g., $\alpha := [\tilde{m}, \tilde{\gamma}, \tilde{k}]$)
2: Measurement of the stochastic parameter α_n of the n-th sample ($n = 1, \ldots, N$)
3: Estimation of the PDF $p(\alpha)$ for α based on the measurement data $\alpha_1, \alpha_2, \ldots,$ and α_N (see Section IV-B)
4: Definition of the feedback controller $u_L(x, \dot{x})$ as the linear form in (4)
5: Determination of the feedback gains $\breve{k}_g$ and $\breve{\gamma}_g$ by solving the optimization problem (7) (see Section IV-C)
6: Mass production of the nanomechanical system employing the feedback controller $u_L(x, \dot{x}) = \breve{k}_g x + \breve{\gamma}_g \dot{x}$

Section IV-C explains the approach to solving the optimization problem (7). The vibrations of the devices are controlled using linear feedback control inputs in association with the resulting gains. These gains can be preset on the devices during the mass production process, meaning that online tuning of the gain is not required.

B. ESTIMATION OF THE PDF OF THE STOCHASTIC PARAMETER

This section describes our approach to estimating the PDF of the stochastic parameter α. Initially, the values of the stochastic parameters are obtained through measurements of N fabricated samples. This provides the set of measurement data $\{\alpha_1, \alpha_2, \ldots, \alpha_N\}$. The PDF $p(\alpha)$ is estimated using these data in conjunction with a statistical method. In this paper, we focus on the kernel density estimation (KDE) approach, which is a promising method for estimating PDFs [39]. In the following text, the KDE method is briefly reviewed in the case that α is simply a scalar.

Using the Gaussian kernel function $K(z) := (1/\sqrt{2\pi}) \times \exp(-z^2/2)$, the PDF $p(\alpha)$ is:

$$p(\alpha) \approx \frac{1}{Nw_b} \sum_{n=1}^{N} K\left(\frac{\alpha - \alpha_n}{w_b}\right), \quad (-\infty < \alpha < \infty), \tag{8}$$

where w_b is the constant bandwidth determined by an existing method [40, Section 2.4.2]. The PDF in (8) can be extended for a multi-dimensional stochastic parameter α using a multivariate kernel function [39, Chapter 4]. Since the possible stochastic parameters include physical quantities such as length and mass, these are often positive. In this case, we can take the logarithm of (8) to give the following form [39, Section2.10]:

$$p(\alpha) \approx \frac{1}{\alpha N w_b} \sum_{n=1}^{N} K\left(\frac{(\ln \alpha) - (\ln \alpha_n)}{w_b}\right), \quad (0 < \alpha < \infty). \tag{9}$$

In the demonstration in Section V, the PDF is calculated based on (9).

Other statistical methods for estimating the PDF may be employed. When the mathematical model of the PDF is known but the values of parameters included in the model are unknown, the PDF can be obtained by estimating only the values. As an example, if the PDF is known to follow a normal distribution, its mean and variance should be estimated. One may also employ a simple method in which the PDF is regarded as a histogram constructed from the measurement data.

C. SOLVING THE OPTIMIZATION PROBLEM

This section presents the process used to solve the optimization problem (7). If the value of $\int_\alpha p(\alpha)\hat{J}_\alpha(u_L)d\alpha$ in (7) can be obtained for various u_L, the problem is numerically solved in a local optimal sense by utilizing various optimization tools, such as the Nelder-Mead simplex method [41]. Unfortunately, it is typically not feasible to integrate $\int_\alpha p(\alpha)\hat{J}_\alpha(u_L)d\alpha$ in an analytical sense. Thus, to enable the calculation, we approximate this expression using the

numerical integrations:

$$\int_{\alpha} p(\alpha)\hat{J}_{\alpha}(u_{\mathrm{L}})\mathrm{d}\alpha \approx \sum_{s=1}^{S} w_s \hat{J}_{\alpha}(u_{\mathrm{L}})|_{\alpha=\underline{\alpha}_s}, \tag{10}$$

where S is the number of sample parameters $\underline{\alpha}_s$. The values of the sample parameters $\underline{\alpha}_s$ and coefficients w_s are defined depending on the types of approximations such as the trapezoidal rule and the Monte Carlo approximation. In the demonstration in Section V, the well-known trapezoidal rule is used.

The performance index $J_{\alpha}(u)$ in (2) takes a general nonlinear form with respect to the control input u. It should also be noted that the feedback gains obtained from the optimization problem (7) may be different from those obtained by linear and quadratic indices. The index $J_{\alpha}(u)$ is widely acceptable with regard to nanomechanical systems because it can reflect various types of control objectives.

D. STABILITY AND ROBUSTNESS

Here, we first analyze stability of the feedback system (5) based on the work in [37]. Because the oscillator coordinate $x_{\alpha}(t)$ is expected to converge to the periodic solution $\bar{x}_{\alpha}(t)$ to (5), the stability is analyzed for the difference $e_{\alpha}(t) := x_{\alpha}(t) - \bar{x}_{\alpha}(t)$ between them. Using this difference $e_{\alpha}(t)$, the feedback system (5) can be rewritten as:

$$\begin{bmatrix} \dot{e}_{\alpha} \\ \ddot{e}_{\alpha} \end{bmatrix} = A_{\mathrm{cl}} \begin{bmatrix} e_{\alpha} \\ \dot{e}_{\alpha} \end{bmatrix}, \tag{11}$$

$$A_{\mathrm{cl}} := \begin{bmatrix} 0 & 1 \\ -(\tilde{k}+k_{\mathrm{g}})/\tilde{m} & -(\tilde{\gamma}+\gamma_{\mathrm{g}})/\tilde{m} \end{bmatrix}. \tag{12}$$

The eigenvalues of A_{cl} are then:

$$-\frac{\tilde{\gamma}+\gamma_{\mathrm{g}}}{2\tilde{m}} \pm \frac{\sqrt{(\tilde{\gamma}+\gamma_{\mathrm{g}})^2 - 4\tilde{m}(\tilde{k}+k_{\mathrm{g}})}}{2\tilde{m}}. \tag{13}$$

The eigenvalues take negative real numbers if $(\tilde{\gamma}+\gamma_{\mathrm{g}})^2 - 4\tilde{m}(\tilde{k}+k_{\mathrm{g}}) \geq 0$ holds. Otherwise, the real parts of the eigenvalues are $-(\tilde{\gamma}+\gamma_{\mathrm{g}})/2\tilde{m}$ that are also negative. Because the real parts of all the eigenvalues of A_{cl} are negative for any α, the difference e_{α} is asymptotically stable [37, Corollary 1.4.2, Corollary 1.4.3, Theorem 1.4.4], such that:

$$\lim_{t\to\infty} e_{\alpha}(t) = 0. \tag{14}$$

This asymptotic stability indicates that the oscillator coordinate $x_{\alpha}(t)$ converges to the periodic solution $\bar{x}_{\alpha}(t)$ for any α. These analysis and result for a fixed α are provided in [37, Example 2.1.1].

We next analyze robustness of the feedback system (5). In this analysis, we assume that the feedback system (5) is subjected to the disturbance $d(t)$, meaning that:

$$\tilde{m}\ddot{x} + (\tilde{\gamma}+\gamma_{\mathrm{g}})\dot{x} + (\tilde{k}+k_{\mathrm{g}})x = f + d(t). \tag{15}$$

Here, suppose that $d(t)$ is bounded and continuous in the time t and satisfies $0 < \int_0^{\infty} d(t)^2\mathrm{d}t < \infty$. Using the difference $e_{\alpha}(t)$, the disturbed feedback system (15) is rewritten as:

$$\tilde{m}\ddot{e}_{\alpha} + (\tilde{\gamma}+\gamma_{\mathrm{g}})\dot{e}_{\alpha} + (\tilde{k}+k_{\mathrm{g}})e_{\alpha} = d(t). \tag{16}$$

The robustness of (16) can be evaluated based on a popular metric in robust control theory [21, Section 9.2]. This metric is the L_2 gain from d to e_{α} under $e_{\alpha}(0) = 0$. The gain is denoted by $\Gamma(d)$ and defined as:

$$\Gamma(d) := \frac{\left(\int_0^{\infty} e_{\alpha}(t)^2\mathrm{d}t\right)^{1/2}}{\left(\int_0^{\infty} d(t)^2\mathrm{d}t\right)^{1/2}}. \tag{17}$$

The gain $\Gamma(d)$ indicates the ratio of the difference e_{α} to the disturbance d in power. A small L_2 gain implies the high robustness of the feedback system. In contrast, if the gain is infinite, the system is no longer robust. It is well known that $\Gamma(d)$ is bounded from above using the system transfer function G from d to e_{α} as follows [21, Section 9.2]:

$$\Gamma(d) \leq \max_{\hat{\omega}\in\mathbb{R}} \sigma_{\max}(G(j\hat{\omega})), \quad \forall\, d, \tag{18}$$

$$G(j\hat{\omega}) := \frac{1}{\tilde{m}(j\hat{\omega})^2 + (\tilde{\gamma}+\gamma_{\mathrm{g}})(j\hat{\omega}) + (\tilde{k}+k_{\mathrm{g}})}, \tag{19}$$

where $\sigma_{\max}(G(j\hat{\omega}))$ is the maximum singular value of $G(j\hat{\omega})$ and j is the imaginary number. Solving (18) gives

$$\begin{aligned} \Gamma(d) &\leq \max_{\hat{\omega}\in\mathbb{R}} \sqrt{G(-j\hat{\omega})^{\mathrm{T}} G(j\hat{\omega})} \\ &= \max_{\hat{\omega}\in\mathbb{R}} \Big(\tilde{m}^2\hat{\omega}^4 + ((\tilde{\gamma}+\gamma_{\mathrm{g}})^2 - 2\tilde{m}(\tilde{k}+k_{\mathrm{g}}))\hat{\omega}^2 \\ &\quad + (\tilde{k}+k_{\mathrm{g}})^2\Big)^{-1/2} \\ &= \begin{cases} 1/(\tilde{k}+k_{\mathrm{g}}) & ((\tilde{\gamma}+\gamma_{\mathrm{g}})^2 \geq 2\tilde{m}(\tilde{k}+k_{\mathrm{g}})) \\ 2\tilde{m}\Big/\sqrt{(\tilde{\gamma}+\gamma_{\mathrm{g}})^2(4\tilde{m}(\tilde{k}+k_{\mathrm{g}}) - (\tilde{\gamma}+\gamma_{\mathrm{g}})^2)} & \\ \qquad\qquad\qquad\qquad\qquad\qquad \text{(Otherwise)} \end{cases} \\ &< \infty. \end{aligned} \tag{20}$$

Clearly, the gain $\Gamma(d)$ in (20) never goes to infinity. The effect of the disturbance d is bounded by the upper bounds in (20).

The physical meaning of the gain $\Gamma(d)$ in (20) can be understood based on relationships between physical parameters. As an example, the relationship employed in the demonstration in Section V is:

$$(\tilde{\gamma}+\gamma_{\mathrm{g}}) = \frac{\sqrt{\tilde{m}(\tilde{k}+k_{\mathrm{g}})}}{Q}, \tag{21}$$

where $Q > \sqrt{1/2}$ is the quality factor. Substituting the relationship (21) into (20) yields

$$\Gamma(d) \leq \frac{2Q}{(\tilde{k}+k_{\mathrm{g}})\sqrt{(4-Q^{-2})}} < \frac{\sqrt{2}Q}{(\tilde{k}+k_{\mathrm{g}})}. \tag{22}$$

Thus, it is indicated that the gain $\Gamma(d)$ is characterized by the quality factor Q and the spring constant $(\tilde{k}+k_{\mathrm{g}})$. A small Q and/or large $(\tilde{k}+k_{\mathrm{g}})$ value will result in a small value for the gain, i.e., the small effect of the disturbance d.

V. DEMONSTRATION IN NANOSCALE RECEIVERS

In this section, we employ a state-of-the-art nanoscale receiver [11] as a model case to demonstrate the effectiveness of the proposed control method. The structure and working principle of this receiver are briefly reviewed in Section V-A. The proposed control method is applied to the nanoscale receiver in Section V-B. A numerical simulation based on experimental data obtained from CNTs is demonstrated in Section V-C to evaluate the proposed method.

A. REVIEW OF NANOSCALE RECEIVERS

The nanoscale receiver used as a test case [11] is briefly reviewed in this subsection. Using the vibration of a CNT cantilever, the receiver detects a data transmitted via an incoming electric wave. The receiver is composed of a phase detector and demodulator as illustrated in Fig. 3. The incoming wave $E_{\rm in}(t,\theta)$ contains a phase data θ that the receiver attempts to detect. In the phase detector, the incoming wave $E_{\rm in}(t,\theta)$ is converted into a field emission current $I_\alpha(t)$ via the vibration of the CNT. The demodulator extracts the data θ as the signal $D_\alpha(\theta)$ from the current $I_\alpha(t)$. The details of these components are reviewed in the following two parts, while the variables and functions associated with the receiver are provided in Table 1.

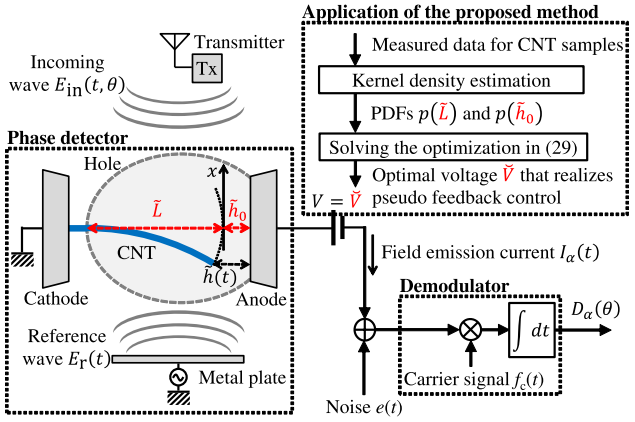

FIGURE 3. Configuration of the nanoscale receiver with the proposed control method applied.

1) PHASE DETECTOR

The incoming electric wave $E_{\rm in}(t,\theta)$ and reference electric wave $E_{\rm r}(t)$ are given as

$$E_{\rm in}(t,\theta) := A\cos(\omega t+\theta) \tag{23}$$

$$E_{\rm r}(t) := bA\cos(\omega t), \tag{24}$$

where A and ω are the amplitude and angular frequency of the waves, respectively. The symbol b is a predefined parameter. The transmitted phase data θ takes θ^+ or θ^- value and corresponds to one bit information.

A charge around the CNT tip is excited by the voltage V applied between the cathode and anode. The CNT tip then vibrates in response to an electric force that is invoked via the Coulomb force associated with the incoming wave $E_{\rm in}$, the reference wave $E_{\rm r}$, and the charge, on the basis of Coulomb's law. This vibration is modeled by (1) with the electric force applied and zero input:

$$\tilde{m}\ddot{x}+\tilde{\gamma}\dot{x}+\tilde{k}x=\tilde{Q}_{\rm ext}(E_{\rm in}(t,\theta)-E_{\rm r}(t)), \tag{25}$$

where x is the coordinate of the CNT tip and $\tilde{Q}_{\rm ext}$ is the charge quantity. The field emission current $I_\alpha(t)$ is approximated by assuming that $x_\alpha(t)$ is sufficiently small, meaning that:

$$I_\alpha(t)\approx\tilde{I}_0+\tilde{I}_1x_\alpha(t)^2, \tag{26}$$

where $\tilde{I}_0$ and $\tilde{I}_1$ are constants.

2) DEMODULATOR

The field emission current $I_\alpha(t)$ is combined with the carrier signal $f_{\rm c}(t)$ in the demodulator. The combined signal, together with the noise component $w_{\rm n}(t)$, is integrated over the focused time T to give:

$$D_\alpha(\theta):=\frac{1}{T}\int_0^T(I_\alpha(t)+w_{\rm n}(t))f_{\rm c}(t){\rm d}t=D_{\alpha,0}(\theta)+D_{\rm n}, \tag{27}$$

where $D_{\alpha,0}(\theta)$ denotes $D_\alpha(\theta)|_{w_{\rm n}(t)=0}$ and T is set to $2\pi s/\omega$ for a predefined natural number s. Using the signal $D_\alpha(\theta)$, an estimate of the phase data θ is obtained between θ^+ and θ^-. If the value of $D_\alpha(\theta)$ is close to that of $D_{\alpha,0}(\theta^+)$, the phase data θ is estimated as θ^+ and vice versa.

B. IMPLEMENTATION FOR NANOSCALE RECEIVERS

Our newly developed control method, as summarized in Fig. 2 and Algorithm 1, is herein applied to the nanoscale receiver reviewed in Section V-A. The intent of the control method is to suppress the effect of the variation of the parameter $\alpha:=[\tilde{L},\tilde{h}_0]$. The key PDFs are shown in Fig. 1(c). The cantilever length $\tilde{L}$ and the gap $\tilde{h}_0$ between the CNT tip and anode were measured in 108 fabricated samples, where discrepant samples had been excluded. The PDFs of both $\tilde{L}$ and $\tilde{h}_0$ were independently determined as $p(\alpha)=p(\tilde{L},\tilde{h}_0)\approx p(\tilde{L})p(\tilde{h}_0)$ using the measured data. The KDE method incorporating the logarithms in (9) was employed to estimate $p(\tilde{L})$ and $p(\tilde{h}_0)$.

The generalized vibration in (1) assumes that the input $u(t)$ used to control the vibration can be applied, whereas the vibration of the CNT in the actual device does not involve such a control input in (25). As an alternative, a simple method of changing the voltage V is possible, because the two parameters $\tilde{k}$ and $\tilde{\gamma}$ affected by manufacturing variation can be tuned by varying the voltage [12]. For a given reference voltage V_0, the associated elasticity and viscosity can be expressed as $\tilde{k}(V)=\tilde{k}(V_0)+\tilde{k}_{\rm g}(V)$ and $\tilde{\gamma}(V)=\tilde{\gamma}(V_0)+\tilde{\gamma}_{\rm g}(V)$, respectively. These expressions are used to insert a pseudo feedback control input to (25) as:

$$\begin{aligned}\tilde{m}\ddot{x}+\tilde{\gamma}(V_0)\dot{x}+\tilde{k}(V_0)x=\tilde{Q}_{\rm ext}(E_{\rm in}(t,\theta)-E_{\rm r}(t))\\-(\tilde{k}_{\rm g}(V)x+\tilde{\gamma}_{\rm g}(V)\dot{x}),\end{aligned} \tag{28}$$

where the force $\tilde{Q}_{\rm ext}(E_{\rm in}(t,\theta)-E_{\rm r}(t))$ depends on the stochastic parameter $\tilde{h}_0$ and the voltage V (see Table 1). In the

TABLE 1. Variables and functions associated with the nanoscale receiver.

Symbols	Meanings	Values/Definitions	References
Environment			
ϵ_0	Electric permittivity in a vacuum	8.854×10^{-12} [F/m]	[11], [12]
CNTs			
ρ	Radius	2.5×10^{-9} [m]	[42]
m_v	Mass per unit volume	$1740[\mathrm{kg/m^3}]$	[43]
m_l	Mass per unit length	$m_\mathrm{v}\pi\rho^2$	—
$\tilde{m}$	Effective mass	$\tilde{L}m_\mathrm{l}/4$	[12]
$\tilde{\gamma}$	Viscosity	$\sqrt{\tilde{m}\tilde{k}}/Q$	[11]
$\tilde{k}$	Elasticity	$2.753(E_\mathrm{u}I_\mathrm{m}/\tilde{L}^3) + 1.162(\tilde{F}_\mathrm{m}/\tilde{L})$	[12]
E_u	Young's modulus	1.0×10^{12} [Pa]	[11], [12]
I_m	Second moment of area	$\pi\rho^4/4$	—
$\tilde{F}_\mathrm{m}$	Tensile force	$\frac{1}{4\pi\epsilon_0}\sum_{a=0}^{\infty}\sum_{b=0}^{\infty}\frac{\tilde{q}_a\tilde{q}_b}{(2(\tilde{h}_0+\rho)-\tilde{\xi}_a-\tilde{\xi}_b)^2}$ where $\tilde{q}_0 := 4\pi\epsilon_0\rho V$, $\tilde{q}_{a+1} := \tilde{q}_a\tilde{\xi}_{a+1}/\rho$, $\tilde{\xi}_0 := 0$, $\tilde{\xi}_{a+1} := \rho^2/(2(\tilde{h}_0+\rho)-\tilde{\xi}_a)$	[12]
Q	Quality factor	3.5	—
Incoming wave			
ω	Angular frequency of the incoming wave	21.3 [MHz] 1)	—
A	Amplitude of the incoming wave	1.0×10^3 [V/m]	—
(θ^+, θ^-)	Phases of the incoming wave	$(0, \pi)$	—
Phase detector			
$\tilde{E}_\mathrm{ext}$	Electromagnetic field between the anode and cathode	$V/(\tilde{L}+\tilde{h}_0)$ 2)	—
V_0	Reference voltage	100 [V]	[11]
b	Coefficient of the reference wave	-2	—
Field emission current			
$\tilde{Q}_\mathrm{ext}$	Amount of charge on the CNT tip	$4\pi\epsilon_0\rho V\sum_{i=0}^{\infty}(\rho/(2\tilde{h}_0))^i$	[11]
$\tilde{I}_0$	Constant used in (26)	$c_1(\pi\rho^2)(\tilde{\varepsilon}(\tilde{h}_0)\tilde{E}_\mathrm{ext})^2\exp\left(-c_2/(\tilde{\varepsilon}(\tilde{h}_0)\tilde{E}_\mathrm{ext})\right)$	[11]
$\tilde{I}_1$	Constant used in (26)	$(-\tilde{I}_0/2\tilde{L}\rho)\left((2/\tilde{\varepsilon}(\tilde{h}_0)) + (c_2/\tilde{\varepsilon}(\tilde{h}_0)^2\tilde{E}_\mathrm{ext})\right)$	[11]
c_1	Constant	3.4×10^{-5} [A/V^2]	[44]
c_2	Constant	7.0×10^{10} [V/m]	[44]
$\tilde{\varepsilon}(\tilde{h})$	Enhancement factor	$3.5 + ((\tilde{L}+\tilde{h}_0-\tilde{h})/\rho)$ 2)	[44]
Demodulator			
$f_\mathrm{c}(t)$	Carrier signal	1	[38]
T	Focused time interval	$5 \times 2\pi/\omega$	—

1) The angular frequency was set to the resonant angular frequency of the oscillator with the mean value of the stochastic parameter α and reference voltage V_0.
2) The distance between the anode and cathode is approximated as $\tilde{L}+\tilde{h}_0$.

following discussion, x obeys (28). The optimal gains $\tilde{k}_\mathrm{g}(\breve{V})$ and $\tilde{\gamma}_\mathrm{g}(\breve{V})$ are obtained at the optimal voltage:

$$\breve{V} := \arg\max_V \int_\alpha p(\alpha)\hat{J}_\alpha(V)\mathrm{d}\alpha. \tag{29}$$

Thus, applying a preset voltage $\breve{V}$ can reduce the effects of manufacturing variation.

To allow calculation of the feedback gain using (29), we determine the performance index $J_\alpha(V)$. Because the receiver is meant to obtain the transmitted binary data accurately, this index should represent the difference between the output currents corresponding to the binary data points [45]. The performance index is given as follows:

$$\begin{aligned} J_\alpha(V) &:= |D_{\alpha,0}(\theta^+) - D_{\alpha,0}(\theta^-)| \\ &= \left|\frac{\tilde{I}_1}{T}\int_0^T (x_\alpha^+(t)^2 - x_\alpha^-(t)^2) f_\mathrm{c}(t)\mathrm{d}t\right|, \end{aligned} \tag{30}$$

where the equality is derived using (26) and (27). The superscripts $+$ and $-$ denote variables/functions corresponding to the binary data points θ^+ and θ^-, respectively. The value of this index can be used as an indicator of the reliability of the data: if the current difference is sufficiently large, the transmitted data should be received correctly.

The proposed method approximates the index $J_\alpha(V)$ in a manner similar to (6), as:

$$\hat{J}_\alpha(V) = \left|\frac{\omega\tilde{I}_1}{2\pi}\int_0^{\frac{2\pi}{\omega}} (\bar{x}_\alpha^+(t)^2 - \bar{x}_\alpha^-(t)^2) f_\mathrm{c}(t)\mathrm{d}t\right|, \tag{31}$$

where $\bar{x}_\alpha(t)$ is the periodic solution to (25) and (28). This approximated index $\hat{J}_\alpha(V)$ is analytically calculated according to the settings in Table 1 [38]. For the motion (28) of the CNT, the stability in (14) and robustness in (22) can be ensured, while the robustness depends on the value of $Q > \sqrt{1/2}$.

C. NUMERICAL RESULTS

We demonstrate the efficacy of the proposed method through a numerical simulation in this section. The proposed method is compared with another control law and a case without control. The parameters of the receiver used in this simulation are summarized in Table 1. The Nelder-Mead simplex method [41] was employed to numerically solve the maximization problem (29) in a local optimal sense. When performing the numerical simulation, it was necessary to calculate the integrals $\int_\alpha p(\alpha)\ldots \mathrm{d}\alpha$, as an example, when solving the maximization problem (29) and when evaluating average performance values. The integrals were approximated using the numerical integration shown in (10) in conjunction with the trapezoidal rule. To avoid outliers, the ranges of $\tilde{L}$ and $\tilde{h}_0$ in the PDFs were limited to [0.6665 μm, 1.5562 μm] and [0.0089 μm, 0.6487 μm], respectively, when performing the numerical integration.

The proposed control method is compared to two other approaches in the simulation. One is deterministic optimal control, in which the performance index with the expected value $\alpha_{\mathrm{E}} := \int_\alpha p(\alpha)\alpha \mathrm{d}\alpha$ of the stochastic parameter (i.e., $\hat{J}_\alpha(V)|_{\alpha=\alpha_{\mathrm{E}}}$) is maximized in the local optimal sense. The other data were acquired without control (i.e., $V = V_0$). The voltages were determined to be 117 V for the deterministic optimal control and 493 V for the proposed optimal control. Below, we evaluate the proposed control method from three perspectives: the control performance for each sample, the associated histogram, and a theoretical analysis regarding the control performance.

Performance evaluation for each sample: Figure 4 shows the numerical results for the performance index $J_\alpha(V)$. These values were obtained from calculations involving 30 CNT samples for which the parameters $\tilde{L}$ and $\tilde{h}_0$ were randomly generated according to the PDFs. The green, blue, and red bars in Fig. 4 indicate the cases without control, with the deterministic optimal control and with the proposed stochastic optimal control, respectively. It is evident that the performance index values for the majority of samples were improved by implementing the proposed stochastic optimal control. The performance values with the sample numbers of 18 and 30 were slightly degraded when using the proposed method. This is believed to have occurred because the proposed method focuses on enhancing the average performance of the samples. Indeed, the average performance value $\int_\alpha p(\alpha)J_\alpha(V)\mathrm{d}\alpha$ was improved by the proposed method. The average values without control, with the deterministic optimal control and with the proposed stochastic optimal control are indicated by green, blue, and red horizontal lines, respectively. It can be seen that the proposed control method increased the average performance.

In Fig. 4, the performance values with the sample numbers of 14 and 15 are well below the others regardless of the control method. Such results are rare due to the extreme values of the stochastic parameters. We subsequently investigated the distributions of the performance values using histograms.

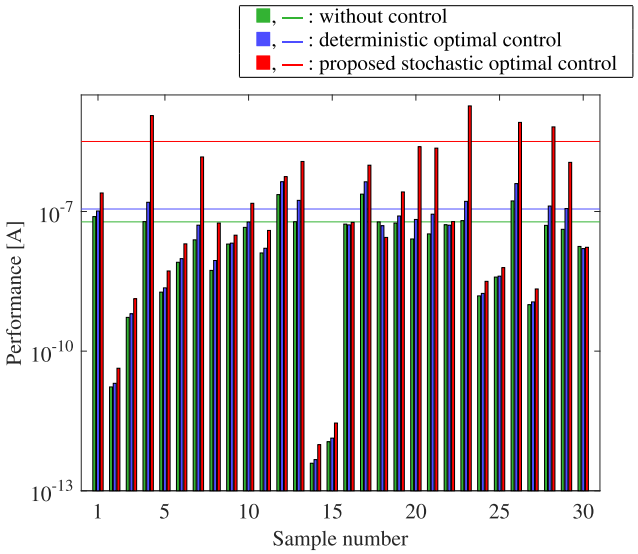

FIGURE 4. The performance of CNT samples. The horizontal lines represent the average performance. The proposed stochastic optimal control produced the best results. The length $\tilde{L}$ and gap $\tilde{h}_0$ of the samples were randomly generated according to the PDFs shown in Fig. 1(c).

Performance evaluation on histograms: We evaluated the distribution of the control performance for 10, 000 CNT samples numerically. The parameters $\tilde{L}$ and $\tilde{h}_0$ for these samples were randomly generated according to the PDFs. Figures 5 (a), (b), and (c) show the histograms of the performance in the cases without control, with the deterministic optimal control, and with the proposed stochastic optimal control, respectively. It is evident that the performance is almost less than 1.0×10^{-6} [A] in the cases without control and with the deterministic optimal control. Meanwhile, the performance greater than 1.0×10^{-6} [A] occurred more frequently when employing the proposed method. In addition, although the samples with low performance (less than 1.0×10^{-11} [A]) are found in Fig. 4, Fig. 5 indicates that such samples were rare.

Theoretical analysis of performance bounds: Finally, the control performance was theoretically analyzed to clarify upper bounds of the performance. We derived probabilistic upper bounds by applying Markov inequality [46, Section 2.2.1] to $J_\alpha(V)$ as:

$$\Pr\Big(J_\alpha(V) > J_{\mathrm{ref}}\Big) \leq \min\left\{\frac{\int_\alpha p(\alpha)J_\alpha(V)\mathrm{d}\alpha}{J_{\mathrm{ref}}}, 1\right\}, \quad (32)$$

where $J_{\mathrm{ref}} > 0$ is a reference value. The numerator of the right hand side in (32) is the average performance value that was estimated as shown in Fig.4. The inequality (32) gives the upper bound of the probability that the control performance $J_\alpha(V)$ is greater than each reference value J_{ref}. Figure 6 plots this upper bound. Here, the green, blue, and red lines indicate the cases without control, with the deterministic optimal control, and with the proposed stochastic optimal control, respectively. Figure 6 demonstrates that the control performance is

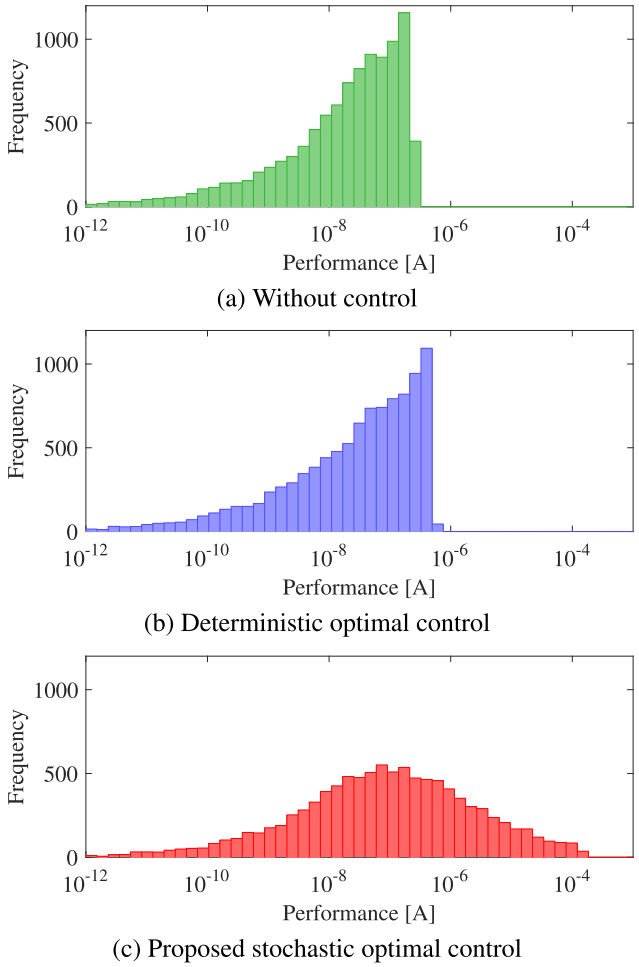

FIGURE 5. Histograms of the performance index $J_\alpha(V)$.

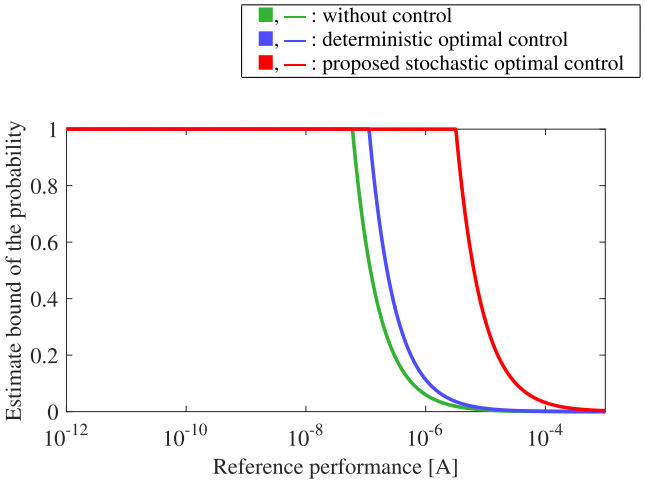

FIGURE 6. Upper bounds of the probability that the performance of a CNT sample is better than the reference performance.

almost less than 1.0×10^{-6} [A] in the cases without control and with the deterministic optimal control. In contrast to these results, the proposed method enhances the performance such that higher values are obtained. These results corresponds to those in Fig. 5: the performance for almost all samples is less than 1.0×10^{-6} [A] in the cases without control and with the deterministic optimal control and is less than 1.0×10^{-4} [A] with the stochastic optimal control. The effectiveness of the proposed method was therefore confirmed by both numerical and theoretical evaluations.

VI. CONCLUSION

In conclusion, this paper presented a novel approach for suppressing the impact of manufacturing variations on the performance of NEMS/MEMS. The stochastic optimal control method enhances the average performance of a system, even with variations in the manufacturing process. The approach described herein requires only the PDF of the stochastic parameter, and the sub-optimal feedback gain in the control loop can be calculated in advance. The effectiveness of the proposed approach was demonstrated via numerical simulations of a nanoscale CNT receiver. The proposed method was found to improve the average performance compared to the results obtained with deterministic control or no control.

In future work, the proposed control approach will be applied to other NEMS/MEMS in conjunction with prototype testing. The proposed method will also be extended to take into account the nonlinearity of the oscillator [13], [47].

APPENDIX: DERIVATION OF AN APPROXIMATION

This appendix presents the process used to derive the approximation in (6). As explained in Section IV-A, the feedback system (5) has a periodic solution $\bar{x}_\alpha(t)$ with the period T_f. Recall the assumption that $\phi(x)$ is continuously differentiable in $x \in \mathbb{R}$. Let $\acute{x}_\alpha(t)$ be a general solution to the homogeneous equation corresponding to (5) such that the solution to (5) reduces to $x_\alpha(t) = \acute{x}_\alpha(t) + \bar{x}_\alpha(t)$. Lagrange's mean value theorem gives:

$$\phi(x_\alpha(t)) = \phi(\bar{x}_\alpha(t)) + \Phi(t)\acute{x}_\alpha(t), \tag{33}$$

$$\Phi(t) := \frac{\partial \phi}{\partial x}(\bar{x}_\alpha(t) + \eta(t)\acute{x}_\alpha(t)), \tag{34}$$

where $\eta(t) \in (0, 1)$ holds. Note that there exists a maximum value of $\Phi(t)$ because $\bar{x}_\alpha(t) + \eta(t)\acute{x}_\alpha(t)$ is bounded and $\partial\phi(x)/\partial x$ is continuous. Because $|\acute{x}_\alpha(t)|$ is bounded by a exponentially decayed function $\acute{a}\exp(-\acute{b}t)$ for some $\acute{a} > 0$ and $\acute{b} > 0$, $|\int_0^T \Phi\acute{x}_\alpha \mathrm{d}t|$ is bounded as:

$$\begin{aligned}\left|\int_0^T \Phi\acute{x}_\alpha \mathrm{d}t\right| &\le \int_0^T |\Phi\acute{x}_\alpha| \mathrm{d}t \\ &\le \int_0^T (\max_t |\Phi(t)|)|\acute{x}_\alpha| \mathrm{d}t \\ &\le (\max_t |\Phi(t)|)\int_0^\infty \acute{a}\exp(-\acute{b}t)\mathrm{d}t \\ &\le (\max_t |\Phi(t)|)(\acute{a}/\acute{b}). \end{aligned} \tag{35}$$

Let us consider the case of $T = sT_f$ for a natural number $s \in \{1, 2, \dots\}$. Using the property (35) yields

$$\begin{aligned} J_\alpha(u_{\mathrm{L}})|_{T=sT_f} - \hat{J}_\alpha(u_{\mathrm{L}}) &= \frac{1}{sT_f}\int_0^{sT_f} \phi(x_\alpha)\mathrm{d}t - \frac{1}{T_f}\int_0^{T_f} \phi(\bar{x}_\alpha)\mathrm{d}t \\ &= \frac{1}{sT_f}\int_0^{sT_f} \left(\phi(\bar{x}_\alpha) + \Phi\acute{x}_\alpha\right)\mathrm{d}t - \frac{1}{sT_f}\int_0^{sT_f} \phi(\bar{x}_\alpha)\mathrm{d}t \\ &= \frac{1}{sT_f}\int_0^{sT_f} \Phi\acute{x}_\alpha \mathrm{d}t \\ &= O(1/s), \quad (s \to \infty). \end{aligned} \tag{36}$$

Therefore, $\hat{J}_\alpha(u_{\mathrm{L}})$ approximates $J_\alpha(u_{\mathrm{L}})$ with an error on the order of $1/s$.

REFERENCES

[1] K. Eom, H. S. Park, D. S. Yoon, and T. Kwon, "Nanomechanical resonators and their applications in biological/chemical detection: Nanomechanics principles," *Phys. Rep.*, vol. 503, no. 4, pp. 115–163, Jun. 2011.

[2] J. Moser, J. Guttinger, A. Eichler, M. J. Esplandiu, D. E. Liu, M. I. Dykman, and A. Bachtold, "Ultrasensitive force detection with a nanotube mechanical resonator," *Nature Nanotechnol.*, vol. 8, no. 7, pp. 493–496, Jun. 2013.

[3] V. Puller, B. Lounis, and F. Pistolesi, "Single molecule detection of nanomechanical motion," *Phys. Rev. Lett.*, vol. 110, no. 12, 2013, Art. no. 125501.

[4] B. E. DeMartini, J. F. Rhoads, M. A. Zielke, K. G. Owen, S. W. Shaw, and K. L. Turner, "A single input-single output coupled microresonator array for the detection and identification of multiple analytes," *Appl. Phys. Lett.*, vol. 93, no. 5, 2008, Art. no. 054102.

[5] K. Y. Fong, M. Poot, and H. X. Tang, "Nano-optomechanical resonators in microfluidics," *Nano Lett.*, vol. 15, no. 9, pp. 6116–6120, 2015.

[6] P. Hosseini, M. Kumar, and H. Bhaskaran, "2-D materials as a functional platform for phase change tunable NEMS," *IEEE Access*, vol. 3, pp. 737–742, 2015.

[7] D. Lei, T. Wang, D. Cao, and J. Fei, "Adaptive dynamic surface control of MEMS gyroscope sensor using fuzzy compensator," *IEEE Access*, vol. 4, pp. 4148–4154, 2016.

[8] A. Yao and T. Hikihara, "Logic-memory device of a mechanical resonator," *Appl. Phys. Lett.*, vol. 105, no. 12, Sep. 2014, Art. no. 123104.

[9] V. Gouttenoire, T. Barois, S. Perisanu, J.-L. Leclercq, S. T. Purcell, P. Vincent, and A. Ayari, "Digital and FM demodulation of a doubly clamped single-walled carbon-nanotube oscillator: Towards a nanotube cell phone," *Small*, vol. 6, no. 9, pp. 1060–1065, 2010.

[10] I. Mahboob, M. Mounaix, K. Nishiguchi, A. Fujiwara, and H. Yamaguchi, "A multimode electromechanical parametric resonator array," *Sci. Rep.*, vol. 4, Mar. 2014, Art. no. 4448.

[11] Y. Tadokoro, Y. Ohno, and H. Tanaka, "Detection of digitally phase-modulated signals utilizing mechanical vibration of CNT cantilever," *IEEE Trans. Nanotechnol.*, vol. 17, no. 1, pp. 84–92, Jan. 2018.

[12] H. Tanaka, T. Ozaki, Y. Ohno, and Y. Tadokoro, "Phase shifter tuned by varying the spring constant of a nanomechanical cantilever," *J. Appl. Phys.*, vol. 122, no. 23, 2017, Art. no. 234501.

[13] Y. Tadokoro, H. Tanaka, and M. I. Dykman, "Driven nonlinear nanomechanical resonators as digital signal detectors," *Sci. Rep.*, vol. 8, Jul. 2018, Art. no. 11284.

[14] S. Ilyas, K. N. Chappanda, and M. I. Younis, "Exploiting nonlinearities of micro-machined resonators for filtering applications," *Appl. Phys. Lett.*, vol. 110, no. 25, 2017, Art. no. 253508.

[15] X. Wei, N. H. Saad, and M. C. L. Ward, "Analysis of manufacturing variation in a coupled microresonators array based on its designed values and measured eigenfrequencies," *IET Micro Nano Lett.*, vol. 5, no. 5, pp. 300–303, Oct. 2010.

[16] N. H. Saad, X. Wei, C. Anthony, H. Ostadi, R. Al-Dadah, and M. C. L. Ward, "Impact of manufacturing variation on the performance of coupled micro resonator array for mass detection sensor," *Procedia Chem.*, vol. 1, no. 1, pp. 831–834, 2009.

[17] L. Schenato, W.-C. Wu, L. El Ghaoui, and K. S. J. Pister, "Process variation analysis for MEMS design," *Proc. SPIE*, vol. 4236, pp. 272–279, Mar. 2001.

[18] K. Funayama, H. Tanaka, J. Hirotani, K. Shimaoka, Y. Ohno, and Y. Tadokoro, "Noise modeling in field emission and evaluation of the nano-receiver in terms of temperature," *IEEE Access*, vol. 7, pp. 57820–57828, 2019.

[19] Y. Ito, K. Fujimoto, Y. Tadokoro, and T. Yoshimura, "On stochastic optimal control for linear systems with robust stability," in *Proc. IEEE 55th Conf. Decis. Control*, Dec. 2016, pp. 5390–5395.

[20] C. Anthony, R. Turnbull, X. Wei, M. Ward, and S. Collins, "Fabrication and quality factor control of a microelectromechanical system resonator with linear differential drive," *IET Sci., Meas. Technol.*, vol. 4, no. 4, pp. 206–213, Jul. 2010.

[21] F. L. Lewis, D. L. Vrabie, and V. L. Syrmos, *Optimal Control*, 3rd ed. Hoboken, NJ, USA: Wiley, 2012.

[22] C. Brif, R. Chakrabarti, and H. Rabitz, "Control of quantum phenomena: Past, present and future," *New J. Phys.*, vol. 12, no. 7, Jul. 2010, Art. no. 075008.

[23] N. Yamamoto, "Coherent versus measurement feedback: Linear systems theory for quantum information," *Phys. Rev. X*, vol. 4, no. 4, 2014, Art. no. 041029.

[24] Y. Kawamura and R. Kanegae, "Mode-selective control of thermal Brownian vibration of micro-resonator (generation of a thermal non-equilibrium state by mechanical feedback control)," *Appl. Phys. Lett.*, vol. 111, no. 13, 2017, Art. no. 133112.

[25] A. Hopkins, K. Jacobs, S. Habib, and K. Schwab, "Feedback cooling of a nanomechanical resonator," *Phys. Rev. B, Condens. Matter*, vol. 68, no. 23, 2003, Art. no. 235328.

[26] J. Fisher and R. Bhattacharya, "Linear quadratic regulation of systems with stochastic parameter uncertainties," *Automatica*, vol. 45, no. 12, pp. 2831–2841, 2009.

[27] R. Bhattacharya, "Robust state feedback control design with probabilistic system parameters," in *Proc. 53rd IEEE Conf. Decis. Control*, Dec. 2014, pp. 2828–2833.

[28] Y. Okura and K. Fujimoto, "A study on robust nonlinear optimal control for parameter variation," in *Proc. IEEE 55th Conf. Decis. Control*, Dec. 2016, pp. 4469–4473.

[29] J.-M. Bismut, "Linear quadratic optimal stochastic control with random coefficients," *SIAM J. Control Optim.*, vol. 14, no. 3, pp. 419–444, 1976.

[30] M. A. Rami and X. Y. Zhou, "Linear matrix inequalities, Riccati equations, and indefinite stochastic linear quadratic controls," *IEEE Trans. Autom. Control*, vol. 45, no. 6, pp. 1131–1143, Jun. 2000.

[31] M. A. Rami, J. B. Moore, and X. Y. Zhou, "Indefinite stochastic linear quadratic control and generalized differential Riccati equation," *SIAM J. Control Optim.*, vol. 40, no. 4, pp. 1296–1311, 2001.

[32] H. Zhang, L. Li, J. Xu, and M. Fu, "Linear quadratic regulation and stabilization of discrete-time systems with delay and multiplicative noise," *IEEE Trans. Autom. Control*, vol. 60, no. 10, pp. 2599–2613, Oct. 2015.

[33] J. Xu, L. Li, and H. Zhang, "Solution to stochastic LQR problem with multiple inputs," *J. Syst. Sci. Complex.*, vol. 30, no. 3, pp. 568–578, 2017.

[34] H. Zhang, Q. Qi, and M. Fu, "Optimal stabilization control for discrete-time mean-field stochastic systems," *IEEE Trans. Autom. Control*, vol. 64, no. 3, pp. 1125–1136, Mar. 2019.

[35] H. Li, J. Xu, and H. Zhang, "Deterministic optimal control of Ito stochastic systems with random coefficients," 2019, *arXiv:1903.00808*. [Online]. Available: https://arxiv.org/abs/1903.00808

[36] S. Schmid, L. G. Villanueva, and M. L. Roukes, *Fundamentals of Nanomechanical Resonators*. Cham, Switzerland: Springer, 2016.

[37] M. Farkas, *Periodic Motions*. New York, NY, USA: Springer-Verlag, 1994.

[38] Y. Ito and Y. Tadokoro, "Simple design on nanoscale receivers using CNT cantilevers," 2019, *arXiv:1904.02529*. [Online]. Available: https://arxiv.org/abs/1904.02529

[39] B. W. Silverman, *Density Estimation for Statistics and Data Analysis*. Boca Raton, FL, USA: CRC Press, 1986.

[40] A. W. Bowman and A. Azzalini, *Applied Smoothing Techniques for Data Analysis: The Kernel Approach with S-Plus Illustrations*. Oxford, U.K.: Oxford Univ. Press, 1997.

[41] J. C. Lagarias, J. A. Reeds, M. H. Wright, and P. E. Wright, "Convergence properties of the Nelder–Mead simplex method in low dimensions," *SIAM J. Optim.*, vol. 9, no. 1, pp. 112–147, 1998.

[42] Y. Sun, D. H. Shin, K. N. Yun, Y. M. Hwang, Y. Song, G. Leti, S.-G. Jeon, J.-I. Kim, Y. Saito, and C. J. Lee, "Field emission behavior of carbon nanotube field emitters after high temperature thermal annealing," *AIP Adv.*, vol. 4, no. 7, 2014, Art. no. 077110.
[43] J. H. Lehman, M. Terrones, E. Mansfield, K. E. Hurst, and V. Meunier, "Evaluating the characteristics of multiwall carbon nanotubes," *Carbon*, vol. 49, no. 8, pp. 2581–2602, 2011.
[44] K. Jensen, J. Weldon, H. Garcia, and A. Zettl, "Nanotube radio," *Nano Lett.*, vol. 7, no. 11, pp. 3508–3511, 2007.
[45] J. G. Proakis, *Digital Communications*. New York, NY, USA: McGraw-Hill, 2001.
[46] C. C. Aggarwal, *Outlier Analysis*, 2nd ed. Cham, Switzerland: Springer, 2017.
[47] Y. Ito, K. Fujimoto, and Y. Tadokoro, "On optimal control based on parametric gradient approximations for nonlinear systems with stochastic parameters," in *Proc. Annu. Amer. Control Conf.*, Jul. 2019, pp. 2936–2941.

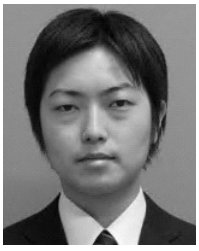

YUJI ITO (M'17) received the B.S., M.S., and Ph.D. degrees from Nagoya University, Aichi, Japan, in 2009, 2011, and 2014, respectively.

Since 2011, he has been with TOYOTA CENTRAL R&D LABS., INC., Japan. His current research interests include stochastic systems theory and nonlinear optimal control.

Dr. Ito is a member of the Society of Instrument and Control Engineers.

KEITA FUNAYAMA received the B.E. and M.E. degrees from Tohoku University, Miyagi, Japan, in 2013 and 2015, respectively, all in mechanical system engineering. He is currently pursuing the Ph.D. degree with Nagoya University.

Since 2015, he has been with TOYOTA CENTRAL R&D LABS., INC., Japan. His current interests include nano-structured mechanical and electronic devices.

JUN HIROTANI received the Ph.D. degree in engineering from Kyushu University, in 2013.

He is currently an Assistant Professor with the Department of Electronics, Nagoya University. His current research interests include nanoscale energy transfer, thermophysical properties of nanomaterials, and flexible electronic devices.

YUTAKA OHNO received the B.E., M.E., and Ph.D. degrees from Nagoya University, Aichi, Japan, in 1995, 1997, and 2000, respectively.

He was a Research Scientist with the Japan Society for the Promotion of Science, in 1999. He became a Research Associate, an Assistant Professor, and an Associate Professor with the Department of Quantum Engineering, Nagoya University, in 2000, 2002, and 2008, respectively, where he became a Professor of the EcoTopia Science Institute, in 2015, and also a Professor of the Institute of Materials and Systems for Sustainability, in 2016. He is currently involved in the explorations of electron transport and optical dynamics in nanocarbon materials, and their applications to novel functional devices.

Dr. Ohno is a member of the Japan Society of Applied Physics, the Physical Society of Japan, the Institute of Electronics, Information and Communication Engineers, the Fullerenes and Nanotubes Research Society, and the American Chemical Society.

YUKIHIRO TADOKORO (M'00–SM'18) received the B.E., M.E., and Ph.D. degrees from Nagoya University, Aichi, Japan, in 2000, 2002, and 2005, respectively, all in information electronics engineering.

Since 2006, he has been with TOYOTA CENTRAL R&D LABS., INC., Japan. He was a Research Scholar with the Department of Physics and Astronomy, Michigan State University, East Lansing, MI, USA, in 2011 and 2012, to study nonlinear phenomena for future applications in signal and information processing fields. Since 2019, he has been a Visiting Professor with the Graduate School of Informatics, Nagoya University. His current research interests include nanoscale wireless communication, noise-related phenomena in nonlinear systems, and their applications in vehicles.

Dr. Tadokoro is a Senior Member of the Institute of Electronic, Information and Communication Engineers, Japan.